Chemical Geology 626 (2023) 121454

Contents lists available at ScienceDirect

Chemical Geology

journal homepage: www.elsevier.com/locate/chemgeo

Identification, distribution and geochemical significance of benzo[*b*]naphthofurans and benzo[*b*]naphthothiophenes in source rocks from the Beibuwan Basin, South China Sea

Xin Wang [a], Meijun Li [a,b,*], Taotao Yang [c], Bang Zeng [a], Yang Shi [d], Xiaoqiang Liu [e], Youjun Tang [f]

[a] State Key Laboratory of Petroleum Resources and Prospecting, College of Geosciences, China University of Petroleum (Beijing), Beijing 102249, China
[b] College of Petroleum, China University of Petroleum (Beijing) at Karamay, Karamay 834000, China
[c] Petrochina Hangzhou Research Institute of Geology, Hangzhou 310023, China
[d] Southern Oil Exploration and Development Company, PetroChina, Haikou 570216, China
[e] College of Chemistry and Environmental Engineering, Sichuan University of Science and Engineering, Zigong 643000, China
[f] Key Laboratory of Exploration Technologies for Oil and Gas Resources, Ministry of Education, College of Resources and Environment, Yangtze University, Wuhan 430100, China

ARTICLE INFO

Editor: Hailiang Dong

Keywords:
Benzo[*b*]naphthofurans
Benzo[*b*]naphthothiophenes
Thermodynamic stability
Maturity indicator
Origin

ABSTRACT

The distribution of benzo[*b*]naphthofurans (BNFs) and benzo[*b*]naphthothiophenes (BNTs) and their geochemical significance have been investigated for a set of delta-lacustrine mudstone samples from the Beibuwan Basin, South China Sea. BNF and BNT isomers in source rock extracts are identified in the *m/z* 218 and *m/z* 234 mass chromatograms of the aromatic fractions, respectively. The relative content of BN12F and BN21T increases as the increasing of burial depth and maturity, which is corresponding to relative higher calculated thermostability among the BNF and BNT isomers. Two maturity parameters, BNFR (abundance of BN12F relative to BN21F) and BNTR (abundance of BN21T relative to BN12T), both correlate well with vitrinite reflectance (Ro %), suggesting that these parameters are potential indicators for assessment of source rock maturity (Ro>0.5%). BNTR is more suitable for the mature stage (Ro<1.0%), as errors in measurement increase in overmature stage due to the low abundance of BN12T. The significant correlation between BNFs and DBF indicates their similar origin, likely an oxic environment with higher plant input. The thermal instability of BNFs at the overmature stage suggests that they may be converted to other compounds at high thermal maturity. The absolute concentrations of BNTs show a growing trend as maturity increases, indicating a thermal origin. BNTs may be generated from phenylnaphthalene isomers by incorporating a sulfur atom into biphenyl during catagenesis. This study achieves a better understanding of the occurrence and significance of BNFs and BNTs in sedimentary organic matter.

1. Introduction

Dibenzothiophenes (DBTs), dibenzofurans (DBFs), and their methylated homologues are important polycyclic aromatic compounds in sedimentary rock extracts and crude oils. DBTs and DBFs have mainly been used in maturation evaluation (Radke, 1988; Willsch and Radke, 1995; Chakhmakhchev et al., 1997; Kruge, 2000; Li et al., 2013a, 2013c, 2014b), depositional environment assessment (Hughes et al., 1995; Li et al., 2013b; Yang et al., 2017), oil-source correlation (Guo et al., 2008; Guo and He, 2009) and hydrocarbon migration tracing (Wang et al., 2004; Li et al., 2008, 2014a, 2018; Fang et al., 2016). Benzo[*b*]naphthofurans (BNFs) and benzo[*b*]naphthothiophenes (BNTs), which contain three benzene rings, are complex hetero-atomic aromatic compounds, found in oils and sedimentary organic matter (Fig. 1). However, the distributions, origins, and geochemical applications of BNFs and BNTs have received less attention than those of DBFs and DBTs.

An unidentified BNF isomer was first detected in coal carbonization products by Shultz et al. (1972). Borwitzky and Schomburg, 1979) and Guillén et al. (1992) detected all BNF isomers in coal tar pitch and its volatiles, but their specific configurations were not determined. These

* Corresponding author at: State Key Laboratory of Petroleum Resources and Prospecting, College of Geosciences, China University of Petroleum (Beijing), Beijing 102249, China.
E-mail address: meijunli@cup.edu.cn (M. Li).

https://doi.org/10.1016/j.chemgeo.2023.121454
Received 19 January 2023; Received in revised form 26 March 2023; Accepted 28 March 2023
Available online 3 April 2023

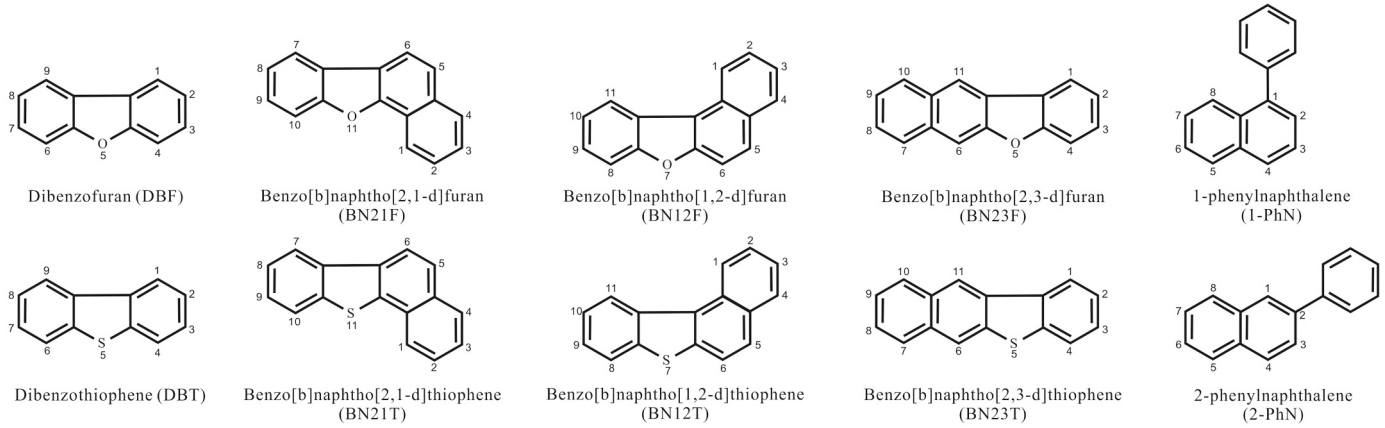

Fig. 1. Structures of benzo[*b*]naphthofurans and benzo[*b*]naphthothiophenes.

compounds have also been found in charcoal from Jurassic wildfires in Poland and Argentina (Marynowski and Simoneit, 2009; Marynowski et al., 2011). They are less soluble in water and less susceptible to (bio) degradation, since their molecules are larger than DBFs (Marynowski and Simoneit, 2009). Li and Ellis (2015) identified BNFs in crude oils and source rocks by co-injection with standard samples. Because of the structural similarities with benzo[*a*]carbazole and benzo[*c*]carbazole, the ratio BN21F/(BN21F + BN12F) was considered to be a potential molecular marker for tracing subsurface hydrocarbon migration (Li and Ellis, 2015).

At present, the origins of these compounds are not clearly understood. Due to their high abundance in coaly shales, BNFs are thought to originate from terrigenous organic matter (Li and Ellis, 2015). Vuković et al. (2016) and Cesar and Grice (2017) suggested that formation of BNFs may also be related to the catalysis of clay minerals. Water and clay minerals released from kerogens react differently with organic matter, which may explain the occurrence of a variety of oxygenated PAHs (Vuković et al., 2016). Because of differences in the behavior of individual BNF isomers in different depositional environments, the BN21F/BN12F ratio can also be used to identify lithofacies (Cesar and Grice, 2017).

Kropp et al. (1994) indicated that BNTs can be generated from benzothiophenes in a microbial degradation environment. The GC retention behavior of BNTs and their alkylated derivatives in different stationary phases has also been reported in previous studies (Mössner et al., 1999). Li et al. (2012, 2014a) identified the three BNT isomers in crude oils by co-injection with authentic internal standards. As benzocarbazoles and BNFs, the BN21T/(BN21T + BN12T) ratio has also been applied to determine oil migration distances (Li et al., 2014a; Fang et al., 2016, 2017). Abundant BN21T were detected in the Niger Delta basin, which may be attributed to a significant marine influence on the depositional environment (Abiodun et al., 2019). Wang et al. (2021) found that the ratios of BN21T/BN12T and BN21T/(BN12T + BN23T) correlated well with maturity in an artificially matured series (Ro > 1.0%). These two parameters can therefore be used for thermal maturity evaluation of overmature sediments.

In previous studies, BNFs and BNTs have been used to trace hydrocarbon migration routes and evaluate thermal maturity in the high to overmature stages (Li et al., 2014a; Li and Ellis, 2015; Fang et al., 2016, 2017; Wang et al., 2021). However, their distributions in immature to mature sediments have not received the same attention, and little is known regarding their origins and formation mechanisms. This study identified all BNF and BNT isomers in source rocks from the Fushan Depression, in the Beibuwan Basin (South China Sea). The purpose of the study is to clarify the thermal evolution behavior of BNFs and BNTs in source rocks. The origins and formation mechanisms of BNFs and BNTs in the geosphere are also preliminarily discussed. It is hoped that this study will contribute to further understanding of the occurrence and sources of BNFs and BNTs in sedimentary organic matter.

2. Methods

2.1. TOC and vitrinite reflectance measurement

Core samples were ground to <80 mesh and carbonates removed with hydrochloric acid prior to analysis. Total organic carbon content (TOC) was measured on a LECO CS-230 Carbon/Sulfur Analyzer. Vitrinite reflectance Ro (%) of the polished blocks was measured using a Leica Model MPV-SP microscopic photometer, following standard procedure (SY/T 5124–2012).

2.2. Rock extract

The powder was extracted in a Soxhlet apparatus for 24 h with 400 ml of dichloromethane and methanol (93:7, v:v) as the solvent. The extracts were dissolved in 50 ml of n-hexane, and insoluble compounds (asphaltenes) were removed by filtering through a funnel with cotton. The residue was separated into saturated and aromatic hydrocarbons by alumina/silica gel columns. The eluents used were 30 ml of n-hexane for the saturated fractions and 30 ml dichloromethane: n-hexane (2:1, v:v) for the aromatic fractions.

2.3. Gas chromatography–mass chromatography (GC–MS)

GC–MS analysis of the aromatic fractions was performed on an Agilent 7890B GC–Agilent 5977A MS system with an HP-5MS fused silica capillary column (60 m × 0.25 mm × 0.25 μm). The initial temperature was 80 °C, which was held for 1 min, then increased to 310 °C at a rate of 3 °C/min, and finally held at 310 °C for 20 min. Helium was used as the carrier gas. The MS was operated in electron ionization (EI) mode with an ionization energy of 70 eV and a scan range of 50–600 Da.

A known quantity of deuterium-substituted phenanthrene (phenanthrene-d_{10}; molecular formula: $C_{14}D_{10}$; molecular mass: 188) was used as an internal standard, and added to each sample before GC–MS analysis. Phenanthrene-d_{10}, which eluted before the phenanthrene, can be identified on the *m/z* 188 mass chromatogram. The peak areas of DBF, DBT, BNFs and BNTs were determined by *m/z* 168, 184, 218, and 234 mass chromatograms, respectively. Their relative concentrations were calculated by correlation with the peak area of phenantharene-d_{10}. The average error of concentration measurement is ±4.5%.

3. Samples and geological setting

A total of 34 source rock samples were collected from the Fushan

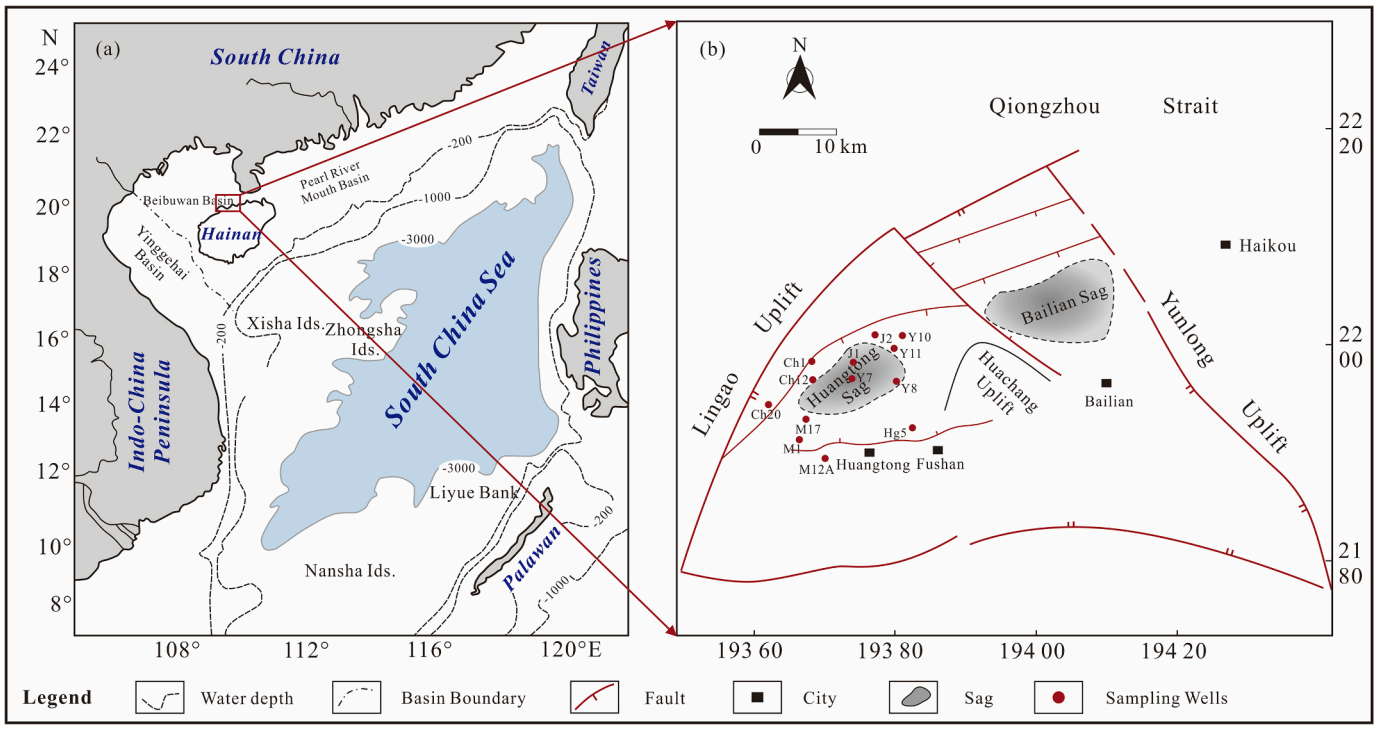

Fig. 2. Location of sedimentary basins in the South China Sea (a) and simplified geological map of the Fushan Depression, Beibuwan Basin (b). The sampling location are shown in Fig. 2(b). (modified after Liu et al., 2021).

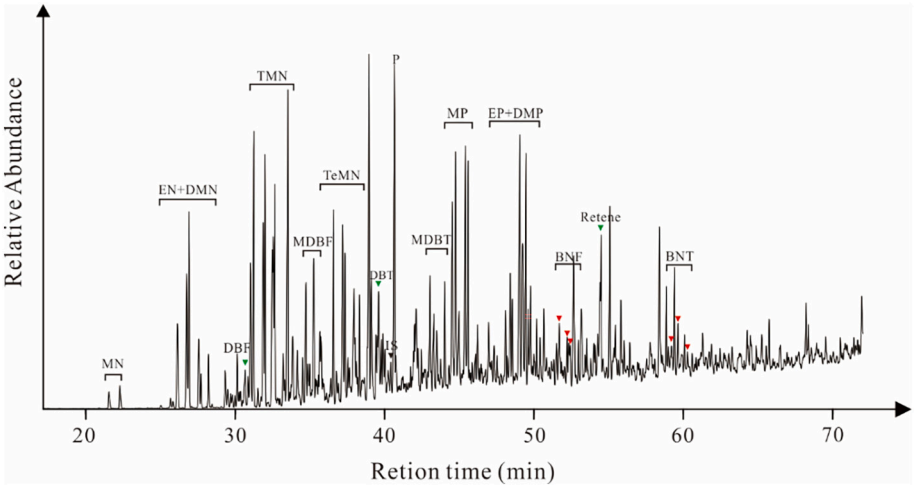

Fig. 3. Representative total ion current chromatogram of the aromatic fractions from source rock extracts. Abbreviations: MN: methylnaphthalene; EN + DMN: ethyl- and dimethylnaphthalene; DBF: dibenzofuran; TMN: trimethylnaphthalene; MDBF: methyldibenzofuran; TeMN: tetramethylnaphthalene; DBT: dibenzothiophene; IS: internal standard; MP: methylphenanthrene; EP + DMP: ethyl- and dimethylphenanthrene; PAHs: polycyclic aromatic hydrocarbons.

Depression, Beibuwan Basin. The Fushan Depression, situated in the southeastern corner of the Beibuwan Basin, is one of a number of Mesozoic-Cenozoic depressions in the northern continental shelf of the South China Sea (Fig. 2). The geological characteristics of the Fushan Depression have been described in detail in previous studies (Liu et al., 2014, 2015; Zeng et al., 2021, 2022).

The Paleogene sequence in the Fushan Depression can be divided into three formations: Changliu, Liushagang, and Weizhou. The Changliu and Weizhou formations are mainly composed of fluvial-alluvial facies. The Liushagang Formation (E*ls*), mainly develops delta-lacustrine facies with an oxidizing environment, which contains the most important source rocks and reservoirs. It is further subdivided into three members (Els_3, Els_2, and Els_1, oldest to youngest). Els_1 and Els_3 generally consist of braided river delta, fan delta, and lacustrine mudstone. The lake level was elevated during deposition of Els_2, resulting in the deposition of enormously thick lacustrine shales, which serve as the main source rocks for the formation.

Abundance of organic matter is relatively high, with average TOC content of 1.60%. The OM is predominantly type II_2 kerogen with relatively high HI values (ranging from 80 to 360 mg HC/g TOC). The vitrinite reflectance of rock samples varies from 0.47% to 1.12%, indicating that the samples are immature to mature. Most of the samples have relatively high Pr/Ph ratios, except for some that were deposited in a suboxic deep-lacustrine environment (Gan et al., 2020; Zeng et al., 2022). Low gammacerane content (average gammacerane/C_{30} hopane ratio of 0.09) indicates a fresh water depositional environment.

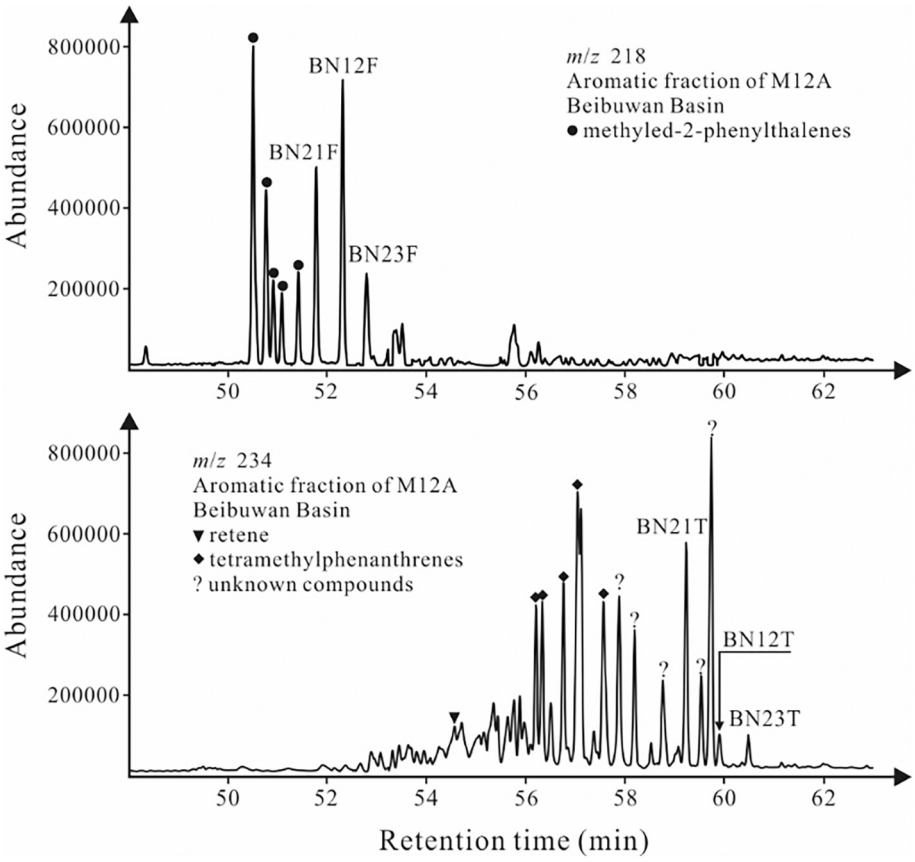

Fig. 4. Identification of benzo[*b*]naphthofurans (m/z 218) and benzo[*b*]naphthothiophenes (m/z 234) in samples from the Fushan Depression, Beibuwan Basin. BNT: benzo[*b*]naphthothiophenes, BNF: benzo[*b*]naphthofurans.

4. Results and discussion

4.1. Occurrence and distribution of benzo[b]naphthofurans and benzo[b] naphthothiophenes

The total ion current (TIC) of the aromatic fractions of the source rock extracts is dominated by a series of alkylnaphthalenes and alkylphenanthrenes (Fig. 3). Dibenzofurans (DBFs), dibenzothiophenes (DBTs), benzo[*b*]naphthofurans (BNFs) and benzo[*b*]naphthothiophenes (BNTs) were all detected in the aromatic fractions, eluting in the sequence: DBF, MDBFs (methyldibenzofuran isomers), DBT, MDBTs (methyldibenzothiophene isomers), BNFs, BNTs.

BNFs are ubiquitous in source rocks and crude oils. They are found in marine, lacustrine, and fluvial/deltaic environments (Li and Ellis, 2015; Li et al., 2023). In a comparison of the retention times shown in *m/z* 218 mass chromatograms of source rocks in this study with those reported in the literature (Li and Ellis, 2015), all BNF isomers have been identified in the sediments of the Fushan Depression (Fig. 4). Li and Ellis (2015) and Cesar and Grice (2017) found that BN23F is present in low concentrations in petroleum fluids. In this study, the content of BN23F was found to be high in samples with vitrinite reflectance (Ro) <0.5%, but decreased dramatically with increasing Ro until the concentration was below the detection limit.

BNTs can also be identified in the *m/z* 234 mass chromatogram (Fig. 4) by comparison with the retention times and elution sequences reported in the literature (Li et al., 2012). Three BNT isomers, i.e. BN21T, BN12T, BN23T were positively identified (Fig. 4). The more stable BN21T isomer predominates over BN12T and BN23T (Wang et al., 2021). BN23T has the lowest concentrations except in a several immature samples.

Table 1
Thermodynamic properties of BNFs and BNTs (The BNF results were modified after Li et al., 2023. The BNT results were modified after Li and Zhang, 2023).

	△E (kcal/mol)	△U (kcal/mol)	△H (kcal/mol)	△G (kcal/mol)
BN12F	0.00	0.00	0.00	0.00
BN21F	0.26	0.26	0.26	0.24
BN23F	1.57	1.57	1.57	1.55
BN21T	0.00	0.00	0.00	0.00
BN23T	2.01	2.00	2.00	2.00
BN12T	3.49	3.57	3.57	2.79

4.2. Thermodynamic stability of benzo[b]naphthofurans and benzo[b] naphthothiophenes

Molecular simulation is an important tool for measuring molecular microstructures and calculating the macro nature of a given system. Quantum chemical calculations were conducted to obtain the thermodynamic parameters of the BNFs and BNTs, including electron energy (ΔE), internal energy (ΔU), enthalpy (ΔH), and Gibbs free energy (ΔG). All the calculations in this study were performed in Gaussian 09 software. Based on density functional perturbation theory, zero-point energy correction was calculated using the B3LYP method, with the frequency of geometric optimization at the 6–311++G (d, p) level (Zhu et al., 2019; Liu et al., 2020).

Analysis of the thermodynamic properties of BNFs shows that BN23F is the least stable isomer with the highest energy. The thermodynamic stabilities of the three BNF isomers are (most to least) BN12F-BN21F-BN23F (Table 1) (Li et al., 2023). Previous studies have suggested that the steric effect is the primary factor affecting the thermal stability of isomers (Yang et al., 2019; Zhu et al., 2019; Liu et al., 2020; Zhu et al.,

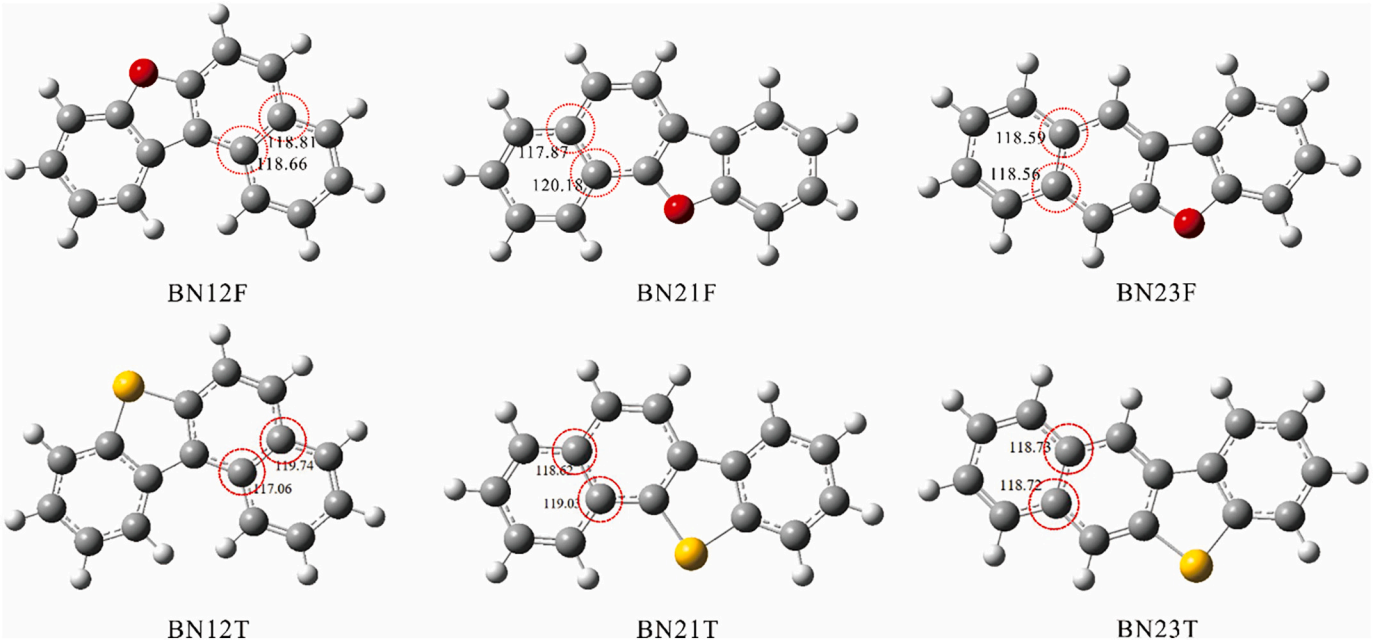

Fig. 5. Geometric optimization of: (a) BN21F, (b) BN12F, (c) BN23F, (d) BN21T, (e) BN12T, (f) BN23T. (The BNF results were modified after Li et al., 2023. The BNT results were modified after Li and Zhang, 2023).

2022). The steric hindrance of the benzene rings at dibenzofuran causes thermodynamic instability. In BN23F, the included angles between the benzene rings and dibenzofuran are considerably deformed from the optimal 120° (Fig. 5), which results in high total energy and poor stability. In contrast, the angles are less deformed in BN12F and BN21F, which are consequently more stable (Li et al., 2023).

BN21T is the most stable of the BNT isomers, with the lowest energy and the least deformation between the benzene rings and dibenzothiophene (Fig. 5). BN23T and BN12T are similar, both having high energy and poor stability (Li and Zhang, 2023).

4.3. *Effects of maturity on the distribution patterns of benzo[b]naphthofurans and benzo[b]naphthothiophenes*

In this study, complete BNT and BNF series were observed in all samples. Maturity of organic matter in source rocks affects the relative abundances of individual BNF and BNT isomers. The distribution patterns of BNFs and BNTs with different maturities are shown in Fig. 6.

There is a marked predominance of BN21F and BN23F over BN12F in immature samples. As maturity increases, the abundance of BN12F increases and eventually exceeds that of BN21F and BN23F. The content of BN23F decreases rapidly, which is consistent with its calculated thermal stability (Table 1). The relative abundance of BN12F and BN21F increased gradually as maturity increases. The relative contents of BNT isomers are also affected by maturity. In the early stage of maturation, the contents of the three BNT isomers are similar. With the thermal maturity increases, the contents of BN12T and BN23T decrease dramatically, probably because of their poor thermal stability (Table 1).

Given the predictability of their distribution patterns with increasing maturity and difference in thermal stability of isomers, BNFR and BNTR (defined as BN12F/BN21F and BN21T/BN12T) have been proposed as maturity indicators (Wang et al., 2021; Li et al., 2023; Li and Zhang, 2023).

To understand the variation of relevant parameters in the actual geological profile, 15 samples from three adjacent wells in the same area were selected to illustrate the continuous changes in BNFR and BNTR with depth (Fig. 7a and Fig. 7b). BNFR is about 0.98 at a depth of 2900 m and increases overall with increasing depth, finally reached 3.0 at approximately 3750 m. Similar variation with depth was also found for BNTR. BNFR increases linearly with depth but BNTR increases slowly at first and then exponentially.

Vitrinite reflectance (%Ro) is an important index reflecting organic matter maturity. Fig. 8 shows the correlations of BNFR and BNTR with measured vitrinite reflectance. The two ratios both correlate positively with vitrinite reflectance ($R^2 = 0.89$ and 0.96, respectively). BNFR and BNTR can therefore be applied as maturity indicators in the immature to mature stages (Ro = 0.4% ~ 1.0%). In thermal simulation experiments, Wang et al. (2021) suggested that BNTR could be used for maturity assessment where Ro>1.0% due to the strong thermal stability of its components. However, it was found in the present study that, at high maturity (Ro>1.0%), the less stable BN21T and BN23T isomers are present in extremely low concentrations or below the detection limit. Assessment of thermal maturity using BNFR is therefore prone to errors, so BNTR is more suitable for maturity assessment where Ro<1.0%.

Despite these correlations, it is still unclear whether maturity is the main controlling factor for BNFR and BNTR. Cesar and Grice (2017) suggested that clay catalysis is a factor in the formation of BN12F and that the ratio BN21F/BN12F is therefore related to depositional environment. Variations in the absolute concentrations of BNF isomers with increasing burial depth are shown in Fig. 9a. The content of each BNF isomer reaches its maximum value around 3070 m, in the sequence BN23F > BN21F > BN12F. With increase in maturity, BN23F content decreases dramatically, with the minimum being close to zero. The absolute concentration of BN12F, on the other hand, reduces slowly, which is attributed to its comparatively higher thermal stability. It is noted that the samples used in Cesar and Grice (2017) were all of low maturity, with Ro = 0.4% ~ 0.6%. In early maturity, the content of each BNF isomer is related to the sedimentary environment and in particular to clay mineral contents. As maturity increases, thermal degradation causes a decrease in the absolute contents of BNF isomers. Previous studies have also shown that the distribution pattern of PAHs is mainly controlled by kinetics at low thermal maturity and by thermodynamics at higher maturity (mainly determined by the stability of compounds) (van Duin et al., 1997; Rospondek et al., 2009). Thus, the relative contents of BNF isomers in the mature stage is controlled by thermal stability, which suggests that BNFR may be a useful indicator at that stage.

Li et al. (2014a) observed that the BN21T/(BN21T + BN12T) ratios of source rocks exhibit no obvious variations with thermal maturity

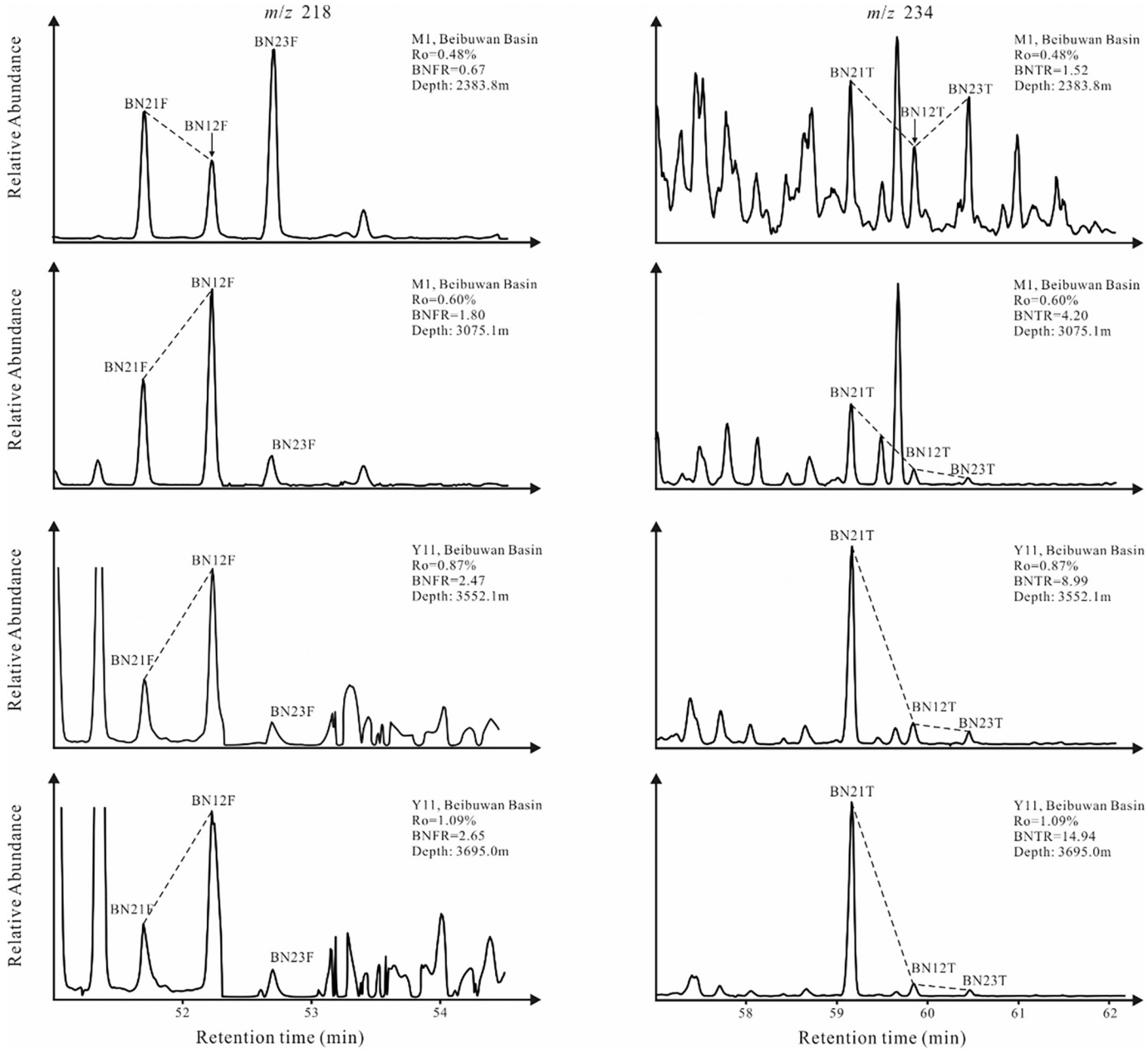

Fig. 6. The effects of thermal maturity on the distributions of benzo[*b*]naphthofuran isomers (*m/z* 218) and benzo[*b*]naphthothiophenes isomers (m/z 234) in the samples from the Fushan Depression.

within the oil-generation window so the ratio has been considered to be an ideal indicator of migration distance. However, there are discrepancies in the thermal stabilities of the three BNT isomers (Wang et al., 2021). The absolute concentration profile of the BNT isomers is shown in Fig. 9b, which indicates that the generation rate of BN21T is significantly higher than that of BN12T and BN23T. The unobvious change in the BN21T/(BN21T + BN12T) ratio observed by Li et al. (2014a) was attributed to low abundance of BN12T, which is explained by its poor thermal stability when Ro > 0.5% (Fig. 6). With increasing maturity, BN21T/(BN21T + BN12T) increases from 0.8 to 0.94, and then stabilizes at close to 1.0 (Fig. 7c), a slight change which has been largely ignored in previous studies. However, it means that the relative contents of BNT isomers can act as migration tracers and maturity indicators based on both maturation-levels and migration fractionation effects.

4.4. Comparison of the distributions of benzo[b]naphthofurans and dibenzofuran

Previous studies have suggested that DBFs originate from polysaccharides, phenols, or woody plants (Born et al., 1989; Pastorova et al., 1994; Sephton et al., 1999; Fenton et al., 2007). Radke et al. (2000) proposed that dibenzofurans in sedimentary rocks may be derived from lichens. However, laboratory experiments indicate that reactions of biphenyls with oxygen form dibenzofurans (Asif et al., 2010). At present, the origins of DBFs in sedimentary rocks remain controversial. Marynowski and Simoneit (2009) proposed that generation of BNFs is related to combustion processes, as they have been found in great quantities in sediments associated with wildfires. They may also originate from unburnt terrestrial material, as implied by their high abundance in immature sedimentary rocks. Li and Ellis (2015) suggested that these oxygenated compounds may derive from terrestrial organic

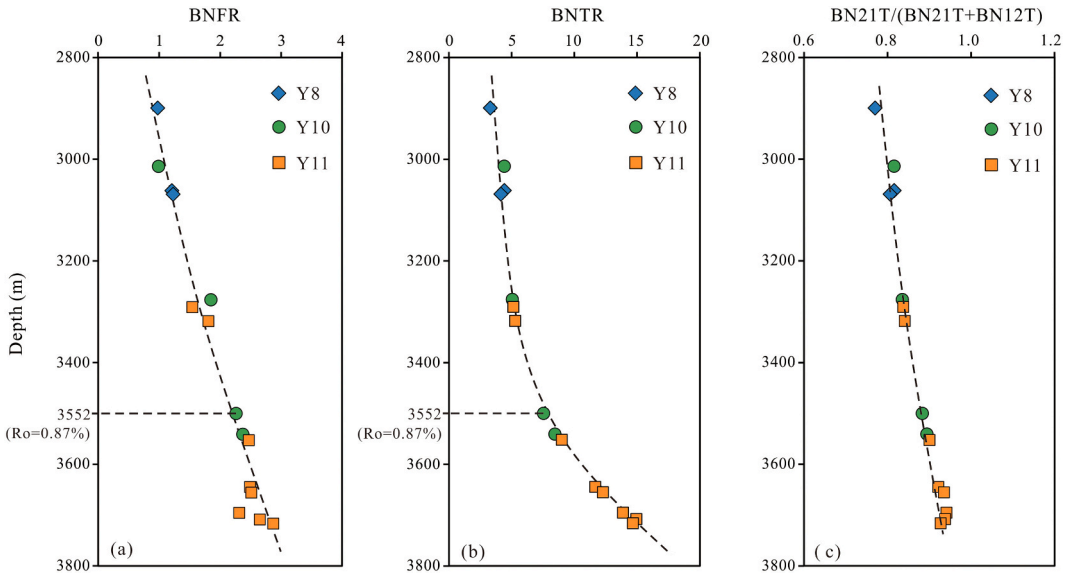

Fig. 7. Variation of (a) BNFR, (b) BNTR and (c) BN21T/(BN21T + BN12T) with depth for source rock samples. (BNFR = BN12F/BN21F; BNTR = BN21T/BN12T).

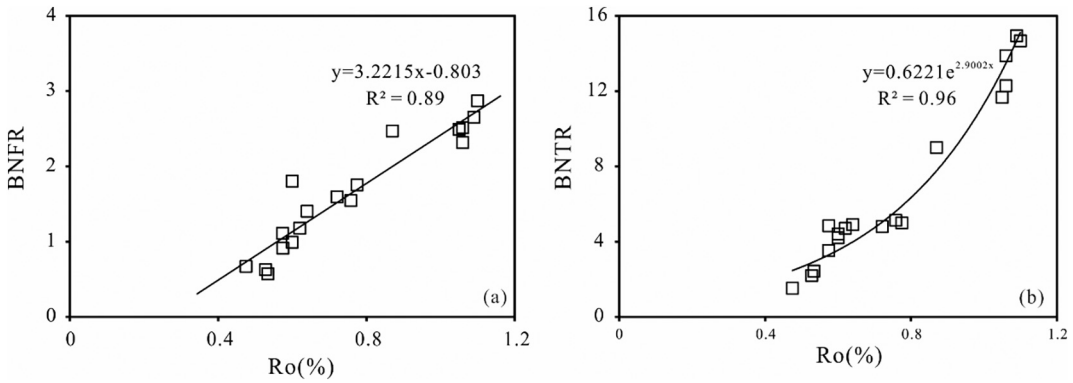

Fig. 8. Variations of (a) BNFR and (b) BNTR with vitrinite reflectance (%Ro) for source rock samples from the Fushan Depression, Beibuwan basin.

matter according to their significant concentrations in coal and coaly shales.

In this study, the absolute concentrations of BNFs were combined with DBF to better understand the formation mechanism of BNFs in the geological samples. The covariation of BNFs with DBF indicates similar origins (Fig. 10a). Although the mechanism of BNF generation is not clear, the similarity between DBFs and BNFs has been preliminarily observed in the geosphere. It has been proposed that an oxic environment is conducive to the formation of DBFs (Li and Ellis, 2015; Pu et al., 1991; Radke et al., 2000). Consequently, an oxic environment with higher plants input can be considered to be favorable for the formation of both DBFs and BNFs.

To gain a better understanding of the origin of BNFs, the relationship between BNF concentrations and vitrinite reflectance was investigated (Fig. 11a). The absolute concentrations of BNFs decrease with increasing maturity. BNFs may therefore be formed during diagenesis, with thermal degradation probably leading to lower concentrations in mature stage. The decrease of BNFs with increasing thermal maturity is consistent with the behavior of another naphthofuran compound, dinaphthofuran (Zhu et al., 2022). This suggests that naphthofuran compounds, BNFs and DNFs, may be generated during diagenesis then become degraded or transformed into other compounds at higher thermal maturity.

4.5. Comparison of the distributions of benzo[b]naphthothiophenes and dibenzothiophene

Previous studies have suggested that sulfur heterocyclic aromatics may be generated by reaction of hydrogen sulfide (H_2S) with unsaturated compounds in sediments during diagenesis (Orr, 1986; Baskin and Peters, 1992; Lu et al., 2013). Reaction of biphenyl and its methylated homologues with elemental sulfur is therefore another possible mechanism for DBT formation (Xia and Zhang, 2002; Asif et al., 2009; Li et al., 2013a, 2013c). In this study, the absolute concentrations of BNTs and DBT were compared to obtain a better understanding of the formation mechanism of BNTs (Fig. 10b). The positive correlation (R^2 = 0.94) suggests that the formation mechanisms of BNTs and DBT are similar.

Cyclized C—S bonds are present in aromatic sulfur compounds such as benzothiophenes (BTs) and dibenzothiophenes (DBTs), which results in high thermal stability (Sinninghe Damste and de Leeuw, 1990). These thermally stable organosulfur compounds are common in mature to overmature oil (Sinninghe Damste and de Leeuw, 1990; Kelemen et al., 2010). In this study, a considerable increase was observed in the absolute concentrations of BNTs with increasing maturity, which indicates that BNTs might be continuously generated in the process of hydrocarbon generation by thermal degradation of kerogen. (Fig. 11b). On the basis of geological observations and laboratory experiments, Asif et al. (2009) suggested that DBT can be generated by biphenyl reacting with sulfur when catalyzed by activated carbon. The analogous studies also

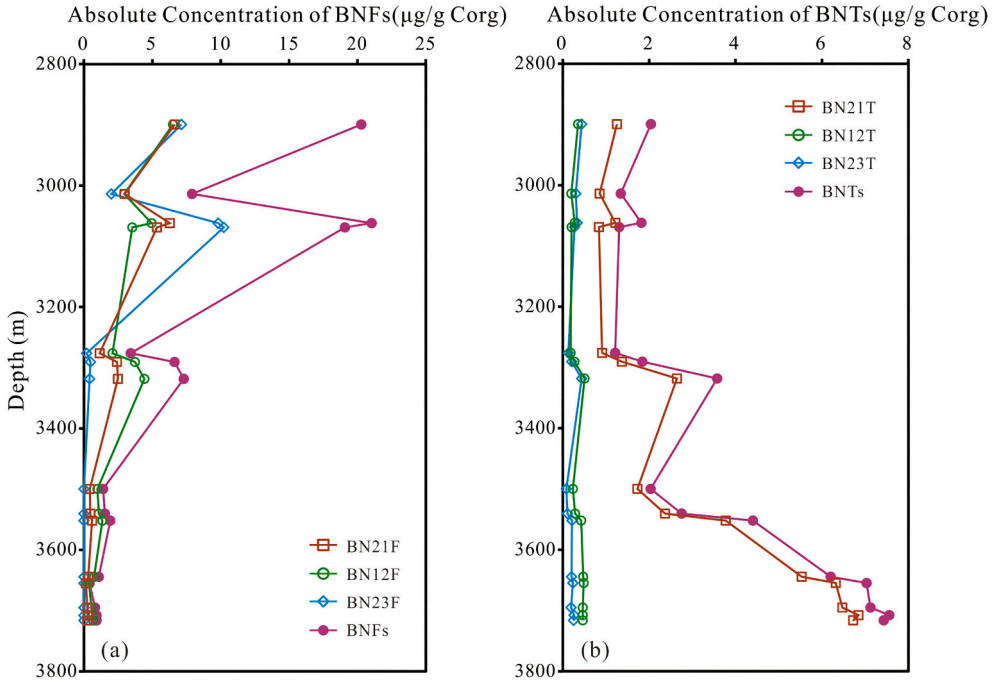

Fig. 9. Variations of absolute concentrations of (a) BNF isomers and (b) BNT isomers with depth for source rock samples.

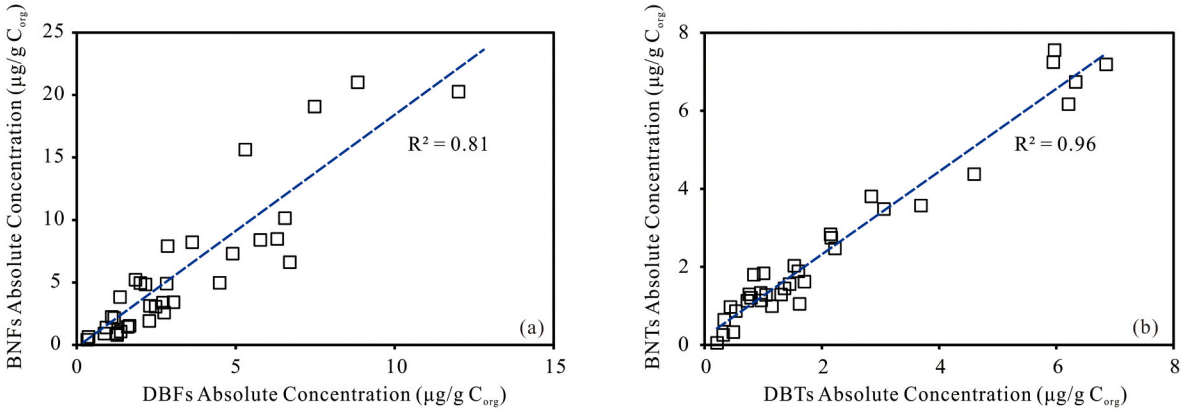

Fig. 10. Cross plots showing the relationships between (a) the absolute concentration of BNFs and DBFs, (b) the absolute concentration of BNTs and DBT.

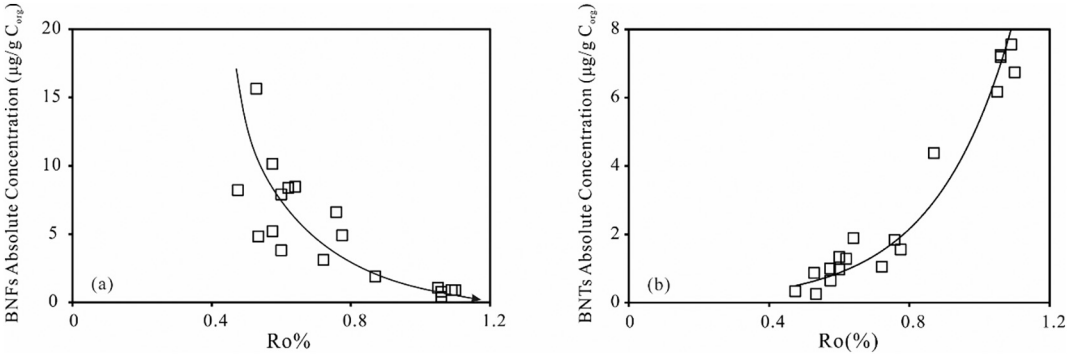

Fig. 11. Cross plots showing the relationships between (a) the absolute concentration of BNFs and vitrinite reflectance (%Ro), (b) the absolute concentration of BNTs and vitrinite reflectance (%Ro).

confirmed that dimethylbiphenyls and trimethylbiphenyls can yield the corresponding dimethyldibenzothiophene and trimethyldibenzothiophene isomers, respectively (Asif et al., 2009; Li et al., 2013a, 2013c). BNTs, as the heteroatomic polycyclic aromatic compounds like DBTs, may have the similar synthesis path. Fig. 12 shows the possible reaction pathways for generation of BNTs from phenylnaphthalene (PhN)

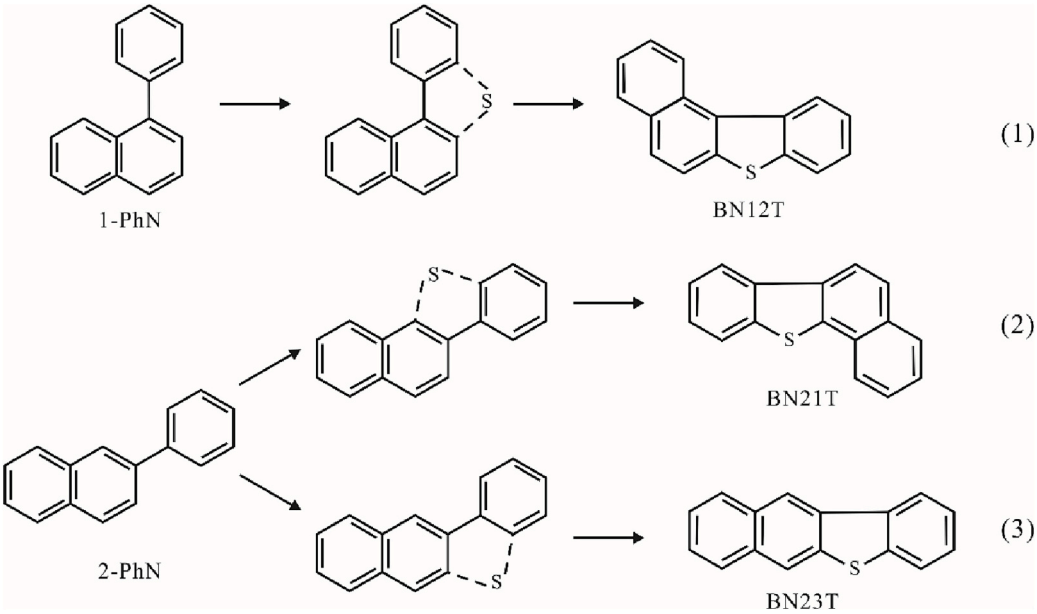

Fig. 12. Tentative scheme of reaction pathways of PhNs to BNTs.

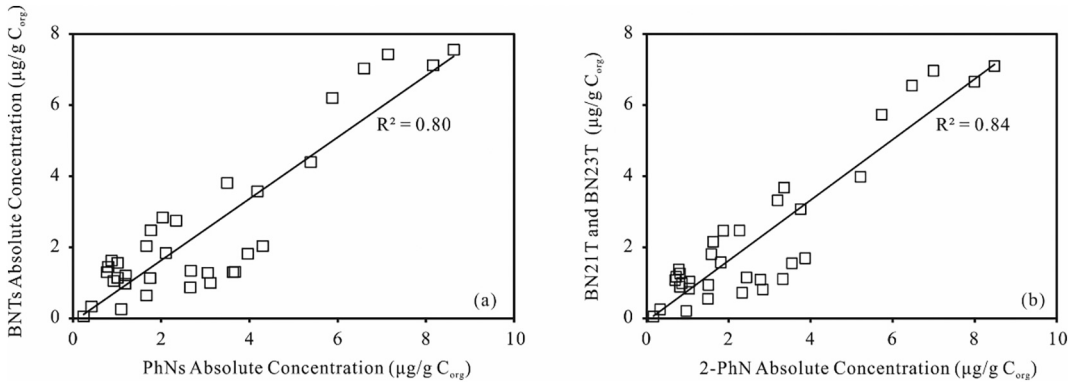

Fig. 13. Cross plots showing the relationships between (a) the absolute concentrations of BNTs and PhNs, (b) the absolute concentrations of BN21T, BN23T and 2-PhN.

isomers. The BN12T isomer can be formed by inserting a sulfur atom into the biphenyl ring system of 1-PhN via reaction pathway (1). Similarly, BN21T and BN23T can be formed from 2-PhN via pathways (2) and (3), respectively (Fig. 12).

4.6. The distribution relationships between PhNs and BNTs

The significant relationship between the concentrations of BNTs and PhNs ($R^2 = 0.80$), as well as between BN21T + BN23T and 2-PhN ($R^2 = 0.84$), may indicate product–precursor links (Fig. 13). Li et al. (2016) indicated that initial formation of 1-PhN—which is thermodynamically less stable—results in low abundance of 1-PhN at lower maturation levels, which may explain the poor correlation between 1-PhN and BN12T.

Fig. 14 shows variations in the concentrations of PhNs and BNT isomers with burial depth. The absolute concentration of BNTs is generally lower than 2 μg/g at depths below 3500 m, with a rapid increase to 4.40 μg/g at 3550 m (Fig. 14a). The values keep increasing until they reach a maximum of 7.50 μg/g at a depth of 3710 m. Due to the paucity of geological samples, the absolute concentrations of BNTs change with depths over 3800 m cannot be observed visually. The concentration of PhNs displays a roughly parallel depth variation trend to that of BNTs. The changes in BN21T + BN23T content with depth are also similar to those of 2-PhN (Fig. 14a). Concentrations of 1-PhN and BN12T are much lower than those of the other isomers, but the variation trend of BN12T is approximately consistent with that of 1-PhN (Fig. 14b). In addition, the abundance of BN23T is very low compared to BN21T, which may be due to the lower energy of BN21T. 2-PhN is more likely to form BN21T than BN23T since the greater thermodynamic stability of BN21T and the different reaction energies of pathways (2) and (3).

To verify the possibility of the proposed reaction pathway (Fig. 12), the reaction energy of the three reaction pathways were calculated through molecular simulation (Table 2). In the reaction process, two hydrogens on the benzene ring and naphthalene ring are supposed to become free radicals, which collide together and eventually become hydrogen. The calculations show that the three reactions can produce in a positive direction, and 2-PhN → BN21T is the more likely to happen.

It is noted that the source input is one of the important factors affecting the concentration of molecular markers. The C_{27}-C_{28}-C_{29} regular sterane ternary diagram shows that all samples fall into the zone of mixed organic matter sources (Fig. 15). The organic matter source may be not the main factor affecting the occurrence of BNTs. In addition, free radical PAHs phenylation reaction is a major pathway for the formation of phenyl PAHs, which mainly occurs in the interaction of hydrothermal fluid with organic matter in the sedimentary systems (Meyer, 1997,

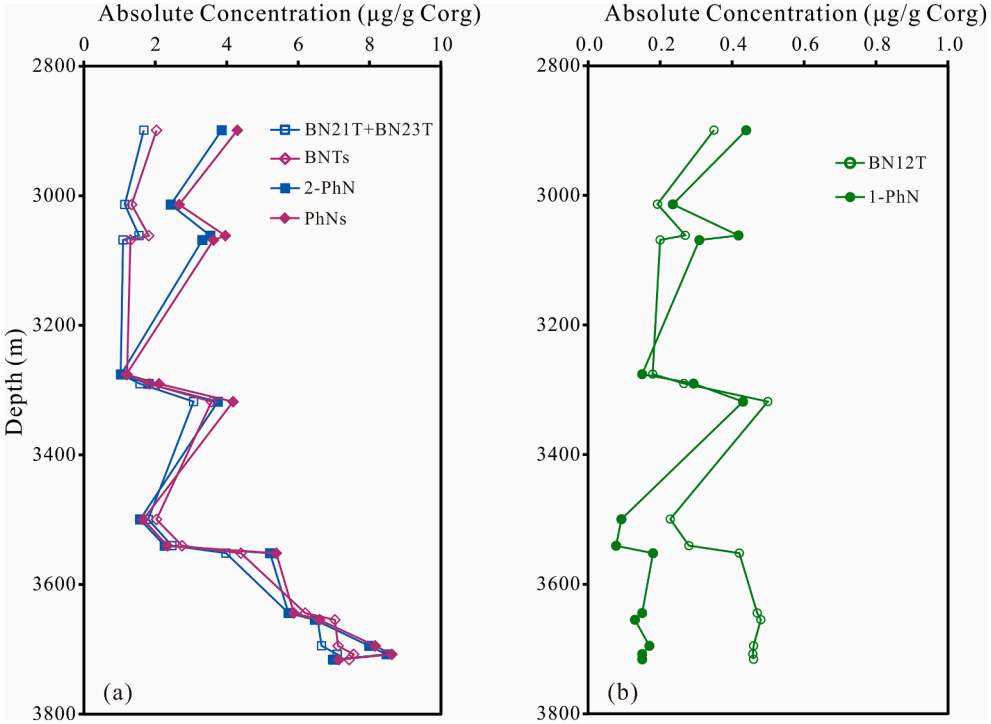

Fig. 14. Variations in the concentrations of BNTs and PhNs with depth for selected rock samples from the Yong'an area.

Table 2
Calculations of reaction energy of the proposed pathways.

	Reaction	Δ_rG_m (kcal/mol)
1	1-PhN + S → BN12T + H_2	−85.87
2	2-PhN + S → BN21T + H_2	−87.20
3	2-PhN + S → BN23T + H_2	−85.19

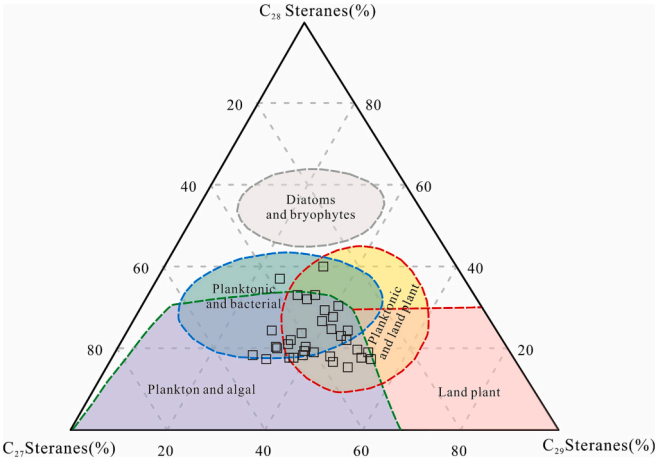

Fig. 15. Ternary diagram of regular steranes (C_{27}, C_{28} and C_{29}) showing the organic matter sources (after Huang and Meinschein, 1979).

2000; Rospondek et al., 2007, 2009). PhNs may not be derived from a specific organic source. The influence of source input on the correlation of PhNs and BNTs can be ignored.

During the process of hydrocarbon generation with the complex geological conditions, one of the possible origins of BNTs was speculated. The content of BNTs and PhNs is also influenced by multiple factors during the complex process of hydrocarbon generation from kerogen. Marynowski et al. (2001) proposed that reductive elimination of sulfur and oxygen in thiophene and furan compounds may result in the formation of PhNs. Consequently, the absolute concentrations of BNTs do not exactly correspond to those of PhNs, in which the content of PhNs is occasionally lower than that of BNTs.

4.7. Effects of depositional environment on the distribution of benzo[b] naphthofurans and benzo[b]naphthothiophenes

BNFs are formed under more oxidizing conditions, while BNTs under more reducing conditions since sulfur is incorporated into the PhN structure (Li and Ellis, 2015). The Pr/Ph ratio of our samples varies from 1.17 to 6.31, suggesting an oxic to sub-oxic depositional environment. To weaken the influence of thermal maturity on the total content of BNFs, the samples with Ro <0.75% were selected to understand the effects of depositional environment on the distribution of BNFs (Fig. 16a). The total content of BNF in oxidizing environment is higher than that in suboxic environment. Thus, the oxidizing environment is conducive to the formation of BNF. Due to BNT is mainly generated during the catagenesis stage, samples with high maturity (Ro >0.75%) was selected to clarify the relationship between depositional environment and BNT content (Fig. 16b). Contrary to BNFs, the content of BNTs in sub-oxic environment is significantly higher than that in oxic environment.

BNT and BNF may be formed at different stages of thermal evolution within different environments (Fig. 17). The delta-lacustrine depositional system developed in Liushagang Formation. The warm and humid climate condition with flourishing vegetation in Paleogene contributes to the input of land plants (Zeng et al., 2022). In the oxidic zone with shallow water depth, the oxidizing environment with abundant terrestrial plants were conducive to the formation of BNF. While BNTs is more likely to be generated in the sub-oxidic zone with deep water depth. As the increase of burial depth and maturity, the sulfur elements originally enriched in the sub-oxidic zone at the bottom of the lacustrine were incorporated to PhNs to form BNTs.

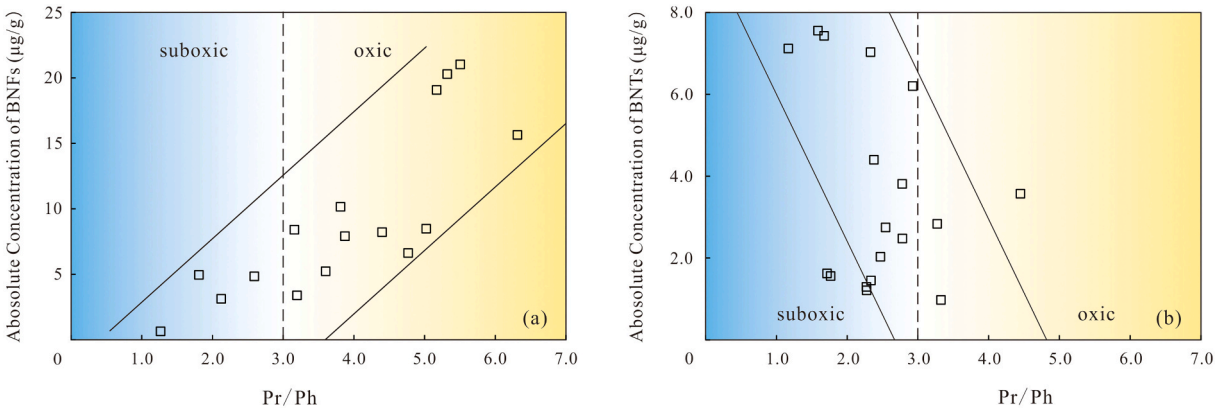

Fig. 16. Cross plots showing the relationships between (a) the absolute concentration of BNFs and Pr/Ph, (b) the absolute concentration of BNTs and Pr/Ph.

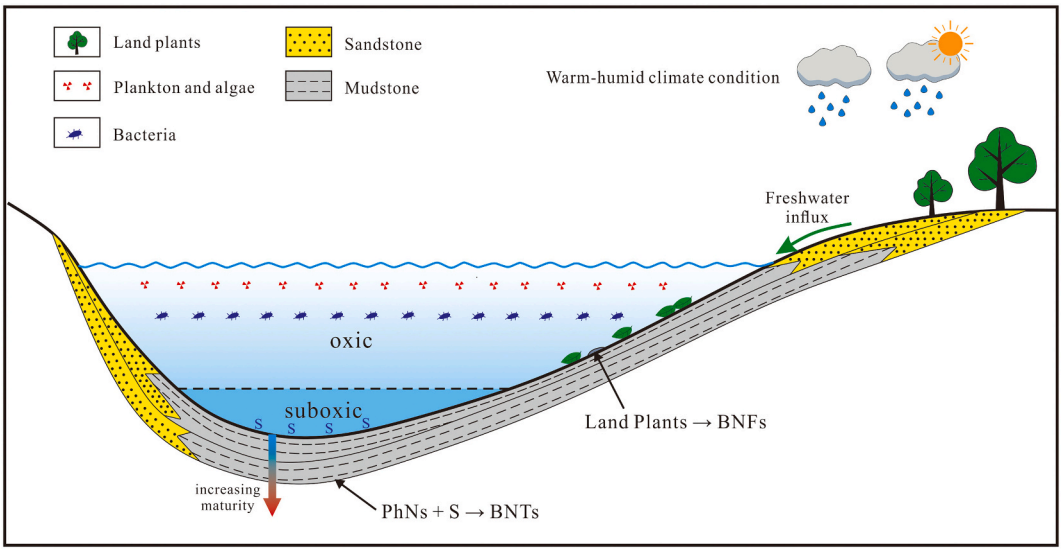

Fig. 17. The formation of BNTs and BNFs in the deposition process.

5. Conclusion

In this study, all BNF and BNT isomers were detected in a series of delta-lacustrine mudstones from the Beibuwan Basin, South China Sea. The effect of maturity on the distribution patterns of BNFs and BNTs in source rock extracts was investigated. The relative abundances of BN12F and BN21T increase gradually with increasing burial depth and maturity. Two maturity ratios, BNFR (BN12F/BN21F) and BNTR (BN21T/BN12T), both have a good correlation with vitrinite reflectance in source rock extracts. These ratios can therefore be applied in maturity assessment of source rocks and oils (Ro>0.5%). BNFR is controlled by sedimentary environment and clay mineral contents during early maturation, while the later is affected by increasing maturity. BNTR is more suitable for maturity assessment in the mature stages (Ro<1.0%), whereas the error would increase in the overmature stage due to low concentrations of BN12T.

The origins of BNFs and BNTs are similar to those of DBFs and DBTs, respectively. An oxic environment with higher plant input is favorable for the generation of BNFs. Since BNF concentrations decrease as maturity increases, BNFs may be generated during diagenesis and converted to other compounds at high thermal maturity.

Unlike BNFs, the absolute concentrations of BNTs generally increase with increasing maturity, indicating a thermal origin. BNTs may be generated from phenylnaphthalene isomers by incorporating a sulfur atom into biphenyl during catagenesis, which is supported by the clear correlation between the concentrations of reactants (PhNs) and products (BNTs).

Declaration of Competing Interest

The authors declare that they have no known competing financial interests or personal relationships that could have appeared to influence the work reported in this paper.

Data availability

Data will be made available on request.

Acknowledgements

This research was financially supported by the National Natural Science Foundation of China (Grant No. 41972148), the South Oil Exploration and Development Company of PetroChina (2020-HNYJ-003). We would also like to thank Shi Shengbao, Zhu Lei, and Zhang Jianfeng of the China University of Petroleum (Beijing) for their assistance and guidance during the experiment. We would also like to thank Editor Hailiang Dong and Dhilip Kumar, as well as two anonymous reviewers whose comments and suggestions helped to improve the quality of the manuscript.

References

Abiodun, B.O., Zhong, N., Oluwadayo, O.S., 2019. The distribution and significance of dimethyldibenzothiophenes, trimethyldibenzothiophenes and benzo[b] naphthothiophenes in source rock extracts from offshore Niger Delta basin. Nigeria. Pet. Sci. Technol. 37, 1978–1986.

Asif, M., Alexander, R., Fazeelat, T., Pierce, K., 2009. Geosynthesis of dibenzothiophene and alkyl dibenzothiophenes in crude oils and sediments by carbon catalysis. Org. Geochem. 40, 895–901.

Asif, M., Alexander, R., Fazeelat, T., Grice, K., 2010. Sedimentary processes for the geosynthesis of heterocyclic aromatic hydrocarbons and fluorenes by surface reactions. Org. Geochem. 41, 522–530.

Baskin, D.K., Peters, K.E., 1992. Early generation characteristics of a sulfur-rich Monterey kerogen. Am. Assoc. Pet. Geol. Bull. 76, 1–13.

Born, J.G.P., Louw, R., Mulder, P., 1989. Formation of dibenzodioxins and dibenzofurans in homogenous gas–phase reactions of phenols. Chemosphere 19, 401–406.

Borwitzky, H., Schomburg, G., 1979. Separation and identification of polynuclear aromatic compounds in coal tar by using glass capillary chromatography including combined gas chromatography-mass spectrometry. J. Chromatogr. A 170, 99–124.

Cesar, J., Grice, K., 2017. The significance of benzo[b]naphtho[d]furans in fluids and source rocks: New indicators of facies type in fluvial-deltaic systems. Org. Geochem. 113, 175–183.

Chakhmakhchev, A., Suzuki, M., Takayama, K., 1997. Distribution of alkylated dibenzothiophenes in petroleum as a tool for maturity assessments. Org. Geochem. 26, 483–489.

Fang, R., Wang, T., Li, M., Xiao, Z., Zhang, B., Huang, S.Y., Shi, S.B., Wang, D., Deng, W., 2016. Dibenzothiophenes and benzo[b]naphthothiophenes: Molecular markers for tracing oil filling pathways in the carbonate reservoir of the Tarim Basin, NW China. Org. Geochem. 91, 68–80.

Fang, R., Li, M., Lü, H., Wang, T., Yuan, Y., Liu, Y., Ni, Z., 2017. Oil charging history and pathways of the Ordovician carbonate reservoir in the Tuoputai region, Tarim Basin, NW China. Pet. Sci. 14, 662–675.

Fenton, S., Grice, K., Twitchett, R., Bottcher, M., Looy, C., Nabbefeld, B., 2007. Changes in biomarker abundances and sulfur isotopes of pyrite across the Permian-Triassic (P/Tr) Schuchert Dal section (East Greenland). Earth Planet. Sci. Lett. 262, 230–239.

Gan, H., Wang, H., Shi, Y., Ma, Q., Liu, E., Yan, D., Pan, Z., 2020. Geochemical characteristics and genetic origin of crude oil in the Fushan sag, Beibuwan Basin, South China Sea. Mar. Pet. Geol. 112, 104114.

Guillén, M.D., Iglesias, M.J., Dominguez, A., Blanco, C.G., 1992. Polynuclear aromatic hydrocarbon retention indices on SE-54 stationary phase of the volatile components of a coal tar pitch Relationships between chromatographic retention and thermal reactivity. J. Chromatogr. A 591, 287–295.

Guo, X., He, S., 2009. Aromatic hydrocarbons as indicators of origin and maturation for light oils from Panyu lower uplift in Pearl River Mouth basin. J. Earth Sci. 20, 824–835.

Guo, X., He, S., Shi, W., 2008. Aromatic geochemistry characteristics of light oils from Panyu Lower Uplift in Pearl River Mouth Basin. Acta Pet. Sin. 29, 52–57 (in Chinese with English abstract).

Huang, W.Y., Meinschein, W.G., 1979. Sterols as ecological indicators. Geochem. Cosmochim. Acta 43, 739–745.

Hughes, W.B., Holba, A.G., Dzou, L.I.P., 1995. The ratios of dibenzothiophene to phenanthrene and pristane to phytane as indicators of depositional environment and lithology of petroleum source rocks. Geochim. Cosmochim. Acta 59, 3581–3598.

Kelemen, S.R., Walters, C.C., Kwiatek, P.J., Freund, H., Afeworki, M., Sansone, M., Lamberti, W.A., Pottorf, R.J., Machel, H.G., Peters, K.E., Bolin, T., 2010. Characterization of solid bitumens originating from thermal chemical alteration and thermochemical sulfate reduction. Geochim. Cosmochim. Acta 74, 5305–5332.

Kropp, K.G., Goncalves, J.A., Andersson, J.T., Fedorak, P.M., 1994. Microbially mediated formation of Benzonaphthothiophenes from Benzo[b]thiophenes. Appl. Environ. Microbiol. 60, 3624–3631.

Kruge, M.A., 2000. Determination of thermal maturity and organic matter type by principal components analysis of the distributions of polycyclic aromatic compounds. Int. J. Coal Geol. 43, 27–51.

Li, M., Ellis, G.S., 2015. Qualitative and quantitative analysis of dibenzofuran, alkyldibenzofurans, and benzo[b]naphthofurans in crude oils and source rock extracts. Energy Fuel 29, 1421–1430.

Li, J., Zhang, Z., 2023. Benzonaphthothiophene: Molecular indicators for thermal maturity. ACS Earth Space Chem. 7, 427–738.

Li, M., Wang, T., Liu, J., Zhang, H., Lu, H., Ma, Q., Gao, L., 2008. Total alkyl dibenzothiophenes content tracing the filling pathway of condensate reservoir in the Fushan Depression, South China Sea. Sci. China Ser. D Earth Sci. 51 (Supp), 138–145.

Li, M., Wang, T., Simoneit, B.R.T., Shi, S., Zhang, L., Yang, F., 2012. Qualitative and quantitative analysis of dibenzothiophene, its methylated homologues, and benzonaphthothiophenes in crude oils, coal, and sediment extracts. J. Chromatogr. A 1233, 126–136.

Li, M., Simoneit, B.R.T., Zhong, N., Fang, R., 2013a. The distribution and origin of dimethyldibenzothiophenes in sediment extracts from the Liaohe Basin, East China. Org. Geochem. 65, 63–73.

Li, M., Wang, T., Zhong, N., Zhang, W., Sadik, A., Li, H., 2013b. Ternary diagram of fluorenes, dibenzothiophenes and dibenzofurans: indicating depositional environment of crude oil source rocks. Energy Explor. Exploit. 31, 569–588.

Li, M., Zhong, N., Shi, S., Zhu, L., Tang, Y., 2013c. The origin of trimethyldibenzothiophenes and their application as maturity indicators in sediments from the Liaohe Basin, East China. Fuel 103, 299–307.

Li, M., Wang, T., Shi, S., Liu, K., Ellis, G.S., 2014a. Benzo[b]naphthothiophenes and alkyl dibenzothiophenes: molecular tracers for oil migration distances. Mar. Pet. Geol. 57, 403–417.

Li, M., Wang, T., Shi, S., Zhu, L., Fang, R., 2014b. Oil maturity assessment using maturity indicators based on methylated dibenzothiophenes. Pet. Sci. 11, 234–246.

Li, M., Wang, H., Shi, S., Fang, R., Tang, Q., Wang, D., 2016. The occurrence and distribution of phenylnaphthalenes, terphenyls and quaterphenyls in selected lacustrine shales and related oils in China. Org. Geochem. 95, 55–70.

Li, M., Liu, X., Wang, T., Jiang, W., Fang, R., Yang, L., Tang, Y., 2018. Fractionation of dibenzofurans during subsurface petroleum migration: based on molecular dynamics simulation and reservoir geochemistry. Org. Geochem. 115, 220–232.

Li, J., Jiang, D., Zhu, Zhi, Yang, P., Zhang, Z., 2023. Effects of thermal maturity of Benzonaphthofurans in coals and its geochemical significance. Acta Sedimentol. Sin. https://doi.org/10.14027/j.issn.1000-0550.2022.146 (In Chinese, published online).

Liu, E., Wang, H., Li, Y., Zhou, W., Leonard, N.D., Lin, Z., Ma, Q., 2014. Sedimentary characteristics and tectonic setting of sublacustrine fans in a half-graben rift depression, Beibuwan Basin, South China Sea. Mar. Pet. Geol. 52, 9–21.

Liu, E., Uysal, I.T., Wang, H., Feng, X., Pan, S., Yan, D., Nguyen, A.D., Zhao, J., 2021. Timing and characterization of multiple fluid flow events in the Beibuwan Basin, northern South China Sea: Implications for hydrocarbon maturation. Mar. Pet. Geol. 123, 104754.

Liu, E., Wang, H., Li, Y., Leonard, N.D., Feng, Y., Pan, S., Xia, C., 2015. Relative role of accommodation zones in controlling stratal architectural variability and facies distribution: Insights from the Fushan Depression, South China Sea. Mar. Pet. Geol. 68, 219–239.

Liu, X., Li, M., Zhang, C., Fang, R., Zhong, N., Xue, Y., Zhou, Y., Jiang, W., Chen, X., 2020. Mechanistic insight into the optimal recovery efficiency of CBM in subbituminous coal through molecular simulation. Fuel 266, 117–137.

Lu, H., Shi, Q., Lu, J., Sheng, G.Y., Peng, P.A., Hsu, C.S., 2013. Petroleum sulfur biomarkers analyzed by comprehensive two-dimensional gas chromatography sulfur-specific detection and mass spectrometry. Energy Fuel 27, 7245–7251.

Marynowski, L., Simoneit, B.R.T., 2009. Widespread upper triassic to lower jurassic wildfire records from Poland: evidence from charcoal and pyrolytic polycyclic aromatic hydrocarbons. Palaios 24, 785–798.

Marynowski, L., Czechowski, F., Simoneit, B.R.T., 2001. Phenylnaphthalenes and polyphenyls in Palaeozoic source rocks of the Holy Cross Mountains, Poland. Org. Geochem. 32, 69–85.

Marynowski, L., Scott, A.C., Zaton, M., Parent, H., Garrido, A.C., 2011. First multi-proxy record of Jurassic wildfires from Gondwana: evidence from the Middle Jurassic of the Neuquen Basin, Argentina. Palaeogeogr., Palaeoclimatol. Palaeoecol. 299, 129–136.

Meyer, R., 1997. Identification of phenyl-substituted polycyclic aromatic compounds in ring furnace gases using GC–MS and GC–AED. Chromatographia 45, 173–182.

Meyer, R., 2000. Phenyl-substituted polycyclic aromatic compounds as intermediate products during pyrolytic reactions involving coal tars, pitches and related materials. Chromatographia 52, 67–76.

Mössner, S.G., Lopez, J.C., Sander, L.C., Lee, M.L., Wise, S.A., 1999. Gas chromatographic retention behavior of polycyclic aromatic sulfur heterocyclic compounds, (dibenzothiophene, naphtho[b]thiophenes, benzo[b] naphthothiophenes and alkyl-substituted derivatives) on stationary phases of different selectivity. J. Chromatogr. A 841, 207–228.

Orr, W.L., 1986. Kerogen asphaltene sulfur relationships in sulfur-rich Monterey oils. Org. Geochem. 10, 499–516.

Pastorova, I., Botto, R.E., Arisz, P.W., Boon, J.J., 1994. Cellulose char structure: a combined analytical Py–GC–MS, FTIR, and NMR study. Carbohydr. Res. 262, 27–47.

Pu, F., Philp, R.P., Li, Z., Yu, X., Ying, G., 1991. Biomarker distributions in crude oils and source rocks from different sedimentary environments. Chem. Geol. 93, 61–78.

Radke, M., 1988. Application of aromatic compounds as maturity indicators in source rocks and crude oils. Mar. Pet. Geol. 5, 224–236.

Radke, M., Vriend, S.P., Ramanampisoa, L.R., 2000. Alkyldibenzofurans in terrestrial rocks: Influence of organic facies and maturation. Geochim. Cosmochim. Acta 64, 275–286.

Rospondek, M.J., Marynowski, L., Góra, M., 2007. Novel arylated polyaromatic thiophenes: phenylnaphtho[b]thiophenes and naphthylbenzo[b]thiophenes as markers of organic matter diagenesis buffered by oxidising solutions. Org. Geochem. 38, 1729–1756.

Rospondek, M.J., Marynowski, L., Chachaj, A., Gora, M., 2009. Novel aryl polycyclic aromatic hydrocarbons: Phenylphenanthrene and phenylanthracene identification, occurrence and distribution in sedimentary rocks. Org. Geochem. 40, 986–1004.

Sephton, M.A., Looy, C.V., Veefkind, R.J., Visscher, H., Brinkhuis, H., de Leeuw, J.W., 1999. Cyclic diaryl ethers in a late Permian sediment. Org. Geochem. 30, 267–273.

Shultz, J.L., Kessler, T., Friedel, R.A., Sharkey, A.G., 1972. High-resolution mass spectrometric investigation of heteroatom species in coal-carbonization products. Fuel 51, 242–246.

Sinninghe Damste, J.S., de Leeuw, J.W., 1990. Analysis, structure and geochemical significance of organically-bound sulphur in the geosphere: State of the art and future research. Org. Geochem. 16, 1077–1101.

van Duin, A.C.T., Baas, J.M.A., van de Graaf, B., de Leeuw, J.W., Bastow, T.P., Alexander, R., 1997. Comparison of calculated equilibrium mixtures of alkylnaphthalenes and alkylphenanthrenes with experimental and sedimentary data; the importance of entropy calculations. Org. Geochem. 26, 275–280.

Vuković, N., Životić, D., Mendonça Filho, J.G., Kravić-Stevović, T., Hámor-Vidó, M., Mendonça, J.D.O., Stojanović, K., 2016. The assessment of maturation changes of humic coal organic matter — Insights from closed-system pyrolysis experiments. Int. J. Coal Geol. 154, 213–239.

Wang, T., He, F., Li, M., Hou, Y., Guo, S., 2004. Alkyldibenzothiophenes: molecular tracers for filling pathway in oil reservoirs. Chin. Sci. Bull. 49, 2399–2404.
Wang, Q., Huang, H., Zheng, L., 2021. Thermal maturity parameters derived from tetra-, penta-substituted naphthalenes and organosulfur compounds in highly mature sediments. Fuel 288, 119626.
Willsch, H., Radke, M., 1995. Distribution of polycyclic aromatic compounds in coals of high rank. Polycycl. Aromat. Compd. 7, 231–251.
Xia, Y., Zhang, G., 2002. Investigation of mechanisms of formation of biphenyls and benzonaphthothiophenes by simulation experiment. Sci. China Ser. D: Earth Sci. 45, 392–398.
Yang, L., Wang, T., Liu, X., Jiang, W., Fang, R., Lai, H., 2017. Phenyldibenzofurans and methyldibenzofurans in source rocks and crude oils, and their implications for maturity and depositional environment. Energy Fuel 31, 2513–2523.
Yang, S., Li, M., Liu, X., Han, Q., Wu, J., Zhong, N., 2019. Thermodynamic stability of methyldibenzothiophenes in sedimentary rock extracts: based on molecular simulation and geochemical data. Org. Geochem. 129, 24–41.
Zeng, B., Li, M., Wang, X., Wang, F., Gong, C., Lai, J., Shi, Y., 2021. Source rock evaluation within a sequence stratigraphic framework of the Palaeogene Liushagang Formation in the Fushan Depression, South China Sea. Geol. J. 57, 2409–2427.
Zeng, B., Li, M., Wang, N., Shi, Y., Wang, F., Wang, X., 2022. Heterogeneous accumulation and geochemical characteristics of organic matter in typical lacustrine basins: a case study of Eocene Liushagang Formation in the Fushan Depression, South China Sea. Pet. Sci. 19, 2533–2548.
Zhu, Z., Li, M., Tang, Y., Qi, L., Leng, J., Liu, X., Xiao, H., 2019. Identification of phenyldibenzothiophenes in coals and the effects of thermal maturity on their distributions based on geochemical data and theoretical calculations. Org. Geochem. 138, 103910.
Zhu, Z., Li, M., Li, J., Qi, L., Liu, X., Xiao, H., Leng, J., 2022. Identification, distribution and geochemical significance of dinaphthofurans in coals. Org. Geochem. 166, 1034399.